Journal of Catalysis 365 (2018) 153–162

Contents lists available at ScienceDirect

Journal of Catalysis

journal homepage: www.elsevier.com/locate/jcat

Towards a greener approach for the preparation of highly active gold/carbon catalyst for the hydrochlorination of ethyne

Jia Zhao *, Bolin Wang, Yuxue Yue, Shuxia Di, Yuanyuan Zhai, Haihua He, Gangfeng Sheng, Huixia Lai, Yihan Zhu, Lingling Guo, Xiaonian Li *

Industrial Catalysis Institute of Zhejiang University of Technology, State Key Laboratory Breeding Base of Green Chemistry-Synthesis Technology, Hangzhou 310014, People's Republic of China

ARTICLE INFO

Article history:
Received 29 May 2018
Revised 29 June 2018
Accepted 30 June 2018

Keywords:
Green preparation
H_2O_2/HCl mixture
Au/AC
Surface chemistry
Ethyne hydrochlorination

ABSTRACT

Gold on activated carbon (Au/AC) materials are promising alternative catalysts for ethyne hydrochlorination. The preparation of active, stable Au/AC catalysts without *aqua regia* for ethyne hydrochlorination remains a significant challenge. A novel catalyst preparation protocol involving impregnation using a H_2O_2/HCl mixture is established for highly active Au/AC catalysts comprising primarily of single-site cationic Au species, as identified by systematic X-ray photoelectron spectroscopy (XPS), temperature-programmed reduction (TPR) analyses and transmission electron microscopy (TEM) imaging. In addition, evaluation of the Au-C interface by temperature-programmed desorption (TPD) analyses showed that the oxidation of activated carbon by the H_2O_2/HCl mixture, which creates surface oxygen-containing functional groups (SOGs), is a crucial step for the formation of active Au/AC catalysts. The structure determination and comprehensive experimental evidence allow density functional theory (DFT) to predict that single-site cationic AuCl species stabilized by SOGs via -O- linkages are efficient active sites for Au-catalyzed ethyne hydrochlorination. In addition, these catalysts can be reused for several times with negligible changes in performance after treatment with the H_2O_2/HCl mixture. The H_2O_2/HCl mixture is thus envisioned as a viable, green alternative to toxic *aqua regia* for the preparation of Au/AC catalysts for ethyne hydrochlorination.

1. Introduction

The potential applications of supported high evenly atomically dispersed gold in the field of catalysis have been widely discussed since Hutchings reported that gold was highly active for ethyne hydrochlorination [1] and Haruta's report of CO oxidation catalyzed by gold dispersed on metal oxides [2]. Generally, the activity of a Au catalysts is frequently discussed in terms of metal dispersion, the perimeter interface between gold and the support and the oxidation states of gold. When the dispersions are high, a greater number of active metal atoms may be expose to the surface, which is accessible to substrates and available for catalysis. In addition, the active species of the gold catalysts are not limited to the metallic state (such as Au^0), and numerous catalytic reactions involved high-valent cationic Au species as the active sites in these Au-based catalysts. For example, for CO oxidation [3] and water-gas shift reactions [4], cationic Au species are more active than metallic Au^0 species. Additionally, the reaction between ethyne and hydrogen chloride for the direct production of the industrially valuable vinyl chloride monomer (VCM) has been extensively studied, and recently, great progress was made in this field [5,6].

Most studies on supported Au catalysts involve the use of metal oxides as supports [7]. Compared with oxide materials, however, carbon materials have many advantages: they have higher chemical stability, and the supported metals can easily be retrieved by burning the carbon materials [8]. In addition, the properties of carbon materials (e.g., the texture properties and the surface chemistry) can easily be adjusted for particular applications [9,10]. Au cationic species can also be stabilized by surface groups of carbon materials, and such stabilized species may serve as the active sites for certain reactions [11]. However, due to the low melting point of Au, the high surface energy of small Au particles and the redox properties of carbon materials, such ultra-small or even atomically dispersed gold containing active cationic species are challenging to synthesize and stabilize on the carbon material support using traditional catalyst preparation methods (e.g., deposition-precipitation and impregnation) [12].

* Corresponding authors.
E-mail addresses: jiazhao@zjut.edu.cn (J. Zhao), xnli@zjut.edu.cn (X. Li).

https://doi.org/10.1016/j.jcat.2018.06.030
0021-9517/

Recently, Hutchings et al. proposed that deposition of $HAuCl_4$ as a precursor onto a carbon support in the presence of *aqua regia* as an impregnation solvent led to considerably active hydrochlorination catalysts because of the formation of single-site cationic Au entities ($AuCl_x$), which act as the active sites in the final material [13,14]. The study also demonstrated that the active species consist of a single-site Au^+ and Au^{3+} cationic species [14]. However, metallic Au^0 species are inactive and are not involving in the reaction [15]. Despite the demonstrated high activity of the Au/C catalyst prepared using *aqua regia*, there are several drawbacks to this technique that make it incompatible with common industrial manufacturing processes. First, *aqua regia* is the origin of toxic NOCl, Cl_2 and NO_x, which would cause serious environmental impacts and limit process safety. Second, the Au/C catalysts made with *aqua regia* are unstable during long reactions due to the dynamic nature of the surface Au species [16]. Finally, the use of the *aqua regia* for the preparation of Au/AC catalysts lead to considerable agglomeration of the gold on the carbon support, which makes it impossible to decreasing the metal loading [17–19]. To circumvent those issues, alternative catalyst preparation methods that are greener and more effective are necessary.

Thus, as a continuation of Hutchings' efforts, we describe an environmentally benign approach using a mixture of hydrogen peroxide and hydrochloric acid (H_2O_2/HCl), i.e., a "green *aqua regia*", which provides facile entry to the production of active Au/AC catalysts and is suitable for practical use. This H_2O_2/HCl mixture was also found to efficiently produce single-site active $AuCl_x$ entities on the carbon support through a combination of the oxidizing effect of the H_2O_2/HCl mixture on the metallic Au^0 species which was related with the reduction property of carbon towards Au^{3+} and the carbon support, which facilitates high-valent and atomically dispersed cationic Au sites. These observations were supported by substantial catalyst characterization studies. Then, the catalytic performances of the prepared Au-based catalysts were investigated in the hydrochlorination of ethyne. In contrast to the catalyst prepared using *aqua regia* (Au/ROX08(AQ)), we demonstrated that the new preparation method using the H_2O_2/HCl mixture leads to catalysts (Au/ROX08(AP)) with improved activity and stability. Mechanistic studies revealed that the surface oxygen-containing functional groups (SOGs) created by the H_2O_2/HCl mixture are better than *aqua regia* at stabilizing single-site cationic Au sites. More importantly, density functional theory (DFT) calculations showed that isolated cationic AuCl entities directly bonded to SOGs (e.g., carbonyl groups) on the carbon support could catalyze the reaction more effectively than AuCl on a graphite surface. In addition, the used catalyst could be efficiently reactivated using H_2O_2/HCl mixture treatment. This strategy allows the green preparation of highly dispersed and active gold/-carbon catalysts.

2. Experimental

2.1. Catalyst preparation

A commercially extruded activated carbon species, Norit ROX08 (surface area of 1100–1200 m^2/g, pore volume of 0.63 cm^3/g, density of 400 g/L, maximum diameter of 0.5 mm, and length of 1–5 mm; ROX08 is a steam-activated carbon that can be thermally reactivated) was used as the catalyst support. First, the ROX08 carbon was ground to obtain a powder (80–100 mesh) and then pretreated with HCl (>36 wt%) to remove residual metal ions (such as trace amounts of K^+ and Al^{3+}). The pretreated ROX08 carbon was filtered, washed with deionized water until the pH of the filtrate was 7, and then dried for use.

A series of carbon-supported Au catalysts were prepared via a wet impregnation method. In a typical synthesis of the 1.0 wt% Au/ROX08(AP) catalyst, 0.6 mL of $HAuCl_4$ (0.05 g_{Au}/mL) aqueous solution was added into 5.4 mL of H_2O_2/HCl mixture (1:3 H_2O_2(30 wt%): HCl (36 wt%)) in a 20 mL flask under magnetic stirring. The solution was stirred for 1 h after complete addition of the $HAuCl_4$ solution. Then, the solution of the gold precursor was added dropwise to 2.97 g of pretreated ROX08 carbon support. The mixture was stirred vigorously for 4 h and then dried at 110 °C under vacuum for 12 h. The synthetic procedures for preparing Au/ROX08(AP) with different Au loadings ranging from 0.1 wt% to 0.5 wt% were similar to that for 1.0 wt% Au/ROX08 (AP), except for the concentration and amount of $HAuCl_4$ solution. $HAuCl_4{\cdot}4H_2O$ solutions in 36 wt% hydrochloric acid or 30 wt% hydrogen peroxide solutions were also prepared to obtain Au catalysts with 1.0 wt% loading. The samples were designated Au/ROX08(A) and Au/ROX08(P), respectively. For comparison, the Au/ROX08(AQ) catalyst was also prepared using *aqua regia* (1:3 HNO_3 (>65 wt%): HCl (>36 wt%)) as solvent in an identical procedure. This catalyst was used as a reference.

The catalysts prepared using deionized water as the solvent on the untreated ROX08 carbon or ROX08 carbon pretreated by the H_2O_2/HCl mixture or *aqua regia* were labeled Au/ROX08-H_2O, Au/ROX08(AP)-H_2O and Au/ROX08(AQ)-H_2O, respectively.

2.2. The regeneration of used Au/ROX08(AP) catalyst

Regeneration treatments of the used catalysts were carried out in a sealed glass vial. In a typical treatment, 2 mL of the H_2O_2/HCl mixture (1:3 H_2O_2: HCl) was prepared in a sealed sample vial. After that, 1 g of the used Au/ROX08(AP) catalyst was added to the mixed solution. The samples were vigorously stirred at 70 °C under ambient pressure for 4 h. After treatment, the samples were dried at 110 °C for 12 h to give the regenerated catalyst, which was labeled Au/ROX08(AP)-R.

2.3. Catalyst characterization and computational procedures

X-ray diffraction (XRD) measurements were carried out on a PANalytical-X'Pert PRO generator with Cu Kα radiation (λ = 0.1541 nm) operating at 60 kV and 55 mA. Diffraction patterns were recorded at a scanning rate of 2° min^{-1} and at a step angle of 0.02°. Transmission electron microscopy (TEM) images were acquired on a Cs-corrected FEI Titan G2 60–300 Microscope operating at 300 kV using an HAADF detector. The solid samples were finely ground and dispersed ultrasonically in ethanol and then transferred to a carbon/Cu grid. Images that clearly reveal single Au atoms were typically recorded at 10 M x direct magnification. Because the nanoparticles and sub-nm species have almost equal chances to be imaged on the support surfaces, the various gold species (>200 total counts) near the edges of the samples in different regions were counted and analyzed. X-ray photoelectron spectroscopy (XPS) was performed with a Kratos AXIS Ultra DLD spectrometer to determine the elemental surface composition of the catalysts. The monochromatized aluminum X-ray source was 1486.6 eV, and the passed energy with an electron analyzer was 40 eV. The pressure in the analysis chamber was lower than 5×10^{-10} Torr during data acquisition. The samples were outgassed under vacuum for 4 h before loading. Binding energies were referred to the C1s line at 284.8 eV. Temperature-programmed reduction (TPR) was performed in a micro-flow reactor fed with hydrogen (10% in Ar) at a flow rate of 45 mL min^{-1}. The temperature was increased from 30 °C to 850 °C at a rate of 10 °C min^{-1}. A thermal conductivity detector (TCD) was used to measure the hydrogen consumption. The integrated TPR signal using CuO as a standard was used to calibrate the TCD. The $AuCl_x$ amount is

calculated as a ratio of the $AuCl_x$ to the total Au amount and the absolute amount in mmol. Surface chemical groups were characterized and quantified by temperature-programmed desorption (TPD). The TPD spectra of CO and CO_2 were obtained with an automated QMS 200 Omnistar system (Pfeiffer Instruments). The samples (100 mg) were set in a quartz tube with a 5 °C min^{-1} linear temperature increase from room temperature to 900 °C, and they were held at 900 °C for 2 h under flowing helium (30 mL min^{-1}). The CO and CO_2 signals were monitored by a quadrupole mass spectrometer. The released CO and CO_2 gasses were calibrated at the end of each measurement. A multiple Gaussian function was applied for spectrum fitting. The numerical calculations were based on a nonlinear routine using the Levenberg-Marquardt method to perform the iterations and make some assumptions, which minimized the sum of the squared deviations. Inductively coupled plasma-mass spectrometry (ICP-MS, PerkinElmer Elan DRC-e) analysis was performed on sample that had been dried using an accurate weighing and digestion process at 160 °C for 12 h.

The first principle calculations in the framework of DFT, including structural and electronic performances, were carried out based on the Cambridge Sequential Total Energy Package known as CASTEP [20,21]. The exchange-correlation functional under the generalized gradient approximation (GGA) [22] with norm-conserving pseudopotentials and the Perdew-Burke-Ernzerhof (PBE) functional was adopted to describe the electron-electron interactions [23]. A kinetic energy cutoff of 750 eV and a Monkhorst-Pack special k-point mesh of 1 × 1 × 10 were proposed for the geometry optimization and electronic structure calculations. During the geometry optimization, all atoms were allowed to relax without any constraints until the convergence thresholds of maximum displacement, maximum force and energy were smaller than 0.001 Å, 0.03 eV/Å and 1.0×10^{-5} eV/atom, respectively. The adsorption energy (ΔE_{abs}) of group A on the surface of the substrate was defined as:

$$\Delta E_{abs} = E * A - (E* + E_A) \quad (1)$$

where *A and * denote the adsorption of group A on the substrate and the bare substrates, and E_A denotes the energy of group A.

2.4. Catalytic test

The catalysts were tested for the hydrochlorination of ethyne in a fixed-bed glass microreactor (i.d. 10 mm). Ethyne (C_2H_2, 10 mL min^{-1}, 1 bar) and hydrogen chloride (HCl, 12 mL min^{-1}, 1 bar) were fed though a mixing vessel to a heated glass reactor containing the catalyst (0.2 g). The total C_2H_2 GHSV is 1480 h^{-1}. The effects of external diffusion were eliminated by application of a flow rate in the range of 10–50 g h mol^{-1} and catalyst loadings between 0.15 and 0.25 g. The reaction rate was not limited by internal mass transport when the grain sizes ranged from 20 to 120 mesh, so the reaction in this study was not affected by internal or external diffusion (Fig. S1). None of the desired product was generated in blank tests at 180 °C using an empty reactor filled with quartz wool. The quartz sand was used to extend the bed length, above and below the catalyst itself, separated by quartz wool. The gas-phase products (ethyne and vinyl chloride) were analyzed online by a gas chromatograph equipped with a flame ionization detector (FID) after NaOH absorption to remove residual hydrogen chloride gas. Chromatographic separation and identification of the products was carried out using a Porapak N packed column (6 ft × 1/800 stainless steel). The peak areas were normalized to investigate the gas-phase products of ethyne hydrochlorination. Given that hydrogen chloride is absorbed by the absorption liquid after the reaction, the volume of the reaction system can be considered constant for the calculations. The amount of 1,2-dichloroethane and chlorinated oligomeric by-products was determined by introducing the reactor outflow into an N-methylpyrrolidone solution and analyzing the obtained N-methylpyrrolidone solution using a Waters GCT Premier chromatograph equipped with an HP-5 capillary column. Product mass fractions were obtained using an internal standard. The conversion of ethyne and the selectivity for VCM were calculated by Eqs. (2) and (3) as follows:

Supplementary data associated with this article can be found, in the online version, at https://doi.org/10.1016/j.jcat.2018.06.030.

$$\text{Acetylene conversion}\,(\%) = \left(1 - \frac{F_A}{F_{A0}}\right) \times 100\% \quad (2)$$

$$\text{VCM Selectivity}\,(\%) = \frac{F_{VCM}}{1 - F_A} \times 100\% \quad (3)$$

where F_{A0}, F_A, and F_{VCM} represent the volume fraction of ethyne in the raw gas, the volume fraction of remaining ethyne, and the volume fraction of vinyl chloride in the product mixture gas, respectively. The carbon balance based on these products was above 98%.

3. Results and discussion

3.1. Au dispersion and chemical state analyses

The morphology and the dispersion of Au particles of Au-based catalysts were investigated, and Fig. 1 shows the STEM images of the Au/ROX08(AP) and Au/ROX08(AQ) catalysts. The fresh Au/ROX08(AQ) catalysts contain large particles ranging from 5 to 12 nm in diameter (Fig. 1a and Fig. S2), which indicates a heterogeneous size distribution among the Au particles that can be easily sintered. This result is consistent with a previous report that showed it is difficult to achieve a high dispersion of Au on carbon materials using traditional wet impregnation methods [13]. In contrast, small particles (diameter <2 nm) are the dominant species in Au/ROX08(AP) (Fig. 1c and Fig. S3); although, some particles (10%) larger than 5 nm in diameter were found on the carbon supports. More importantly, there is a large amount of atomically dispersed gold species presenting on the supports based on the highly magnified image (Fig. 1d). For example, 53% of the gold species counted in the images are presented as isolated atoms on the surface of the Au/ROX08(AP) sample, demonstrating the obvious improvement in the Au dispersion achieved with the developed preparation process. In contrast, the Au/ROX08(AQ) sample consists of large particles and a small number of sub-nm gold clusters, but in some areas, individual atoms are observed (Fig. 1b). In fact, in situ extended X-ray absorption fine structure (EXAFS) and x-ray-absorption near-edge structure (XANES) analysis performed by Hutchings et al. demonstrated that the active sites for ethyne hydrochlorination are the isolated Au cationic species [12]. The atomically dispersed Au species seem to have a significant impact on the catalytic activity in the hydrochlorination reaction. The Au/ROX08 (AP) catalyst, which has a high content of single-site Au species presenting on the carbon support, may be highly active for the hydrochlorination of ethyne. However, isolated Au cationic species are probably not the only condition required for achieving high activity; the carbon surface oxygen groups are also necessary for the active site because graphitic carbon without the SOGs is catalytically inactive [24,25]. These observations are supported by substantial catalyst characterization and theoretical calculations, which we will discuss in detail in the following section.

Elucidating the local and electronic structure of the catalytically active Au-containing species is critical for establishing a structure-activity relationship of the Au/AC catalysts. Detailed characterizations of the Au/ROX08(AQ) and Au/ROX08(AP) samples included XPS analysis. Because more than one Au species

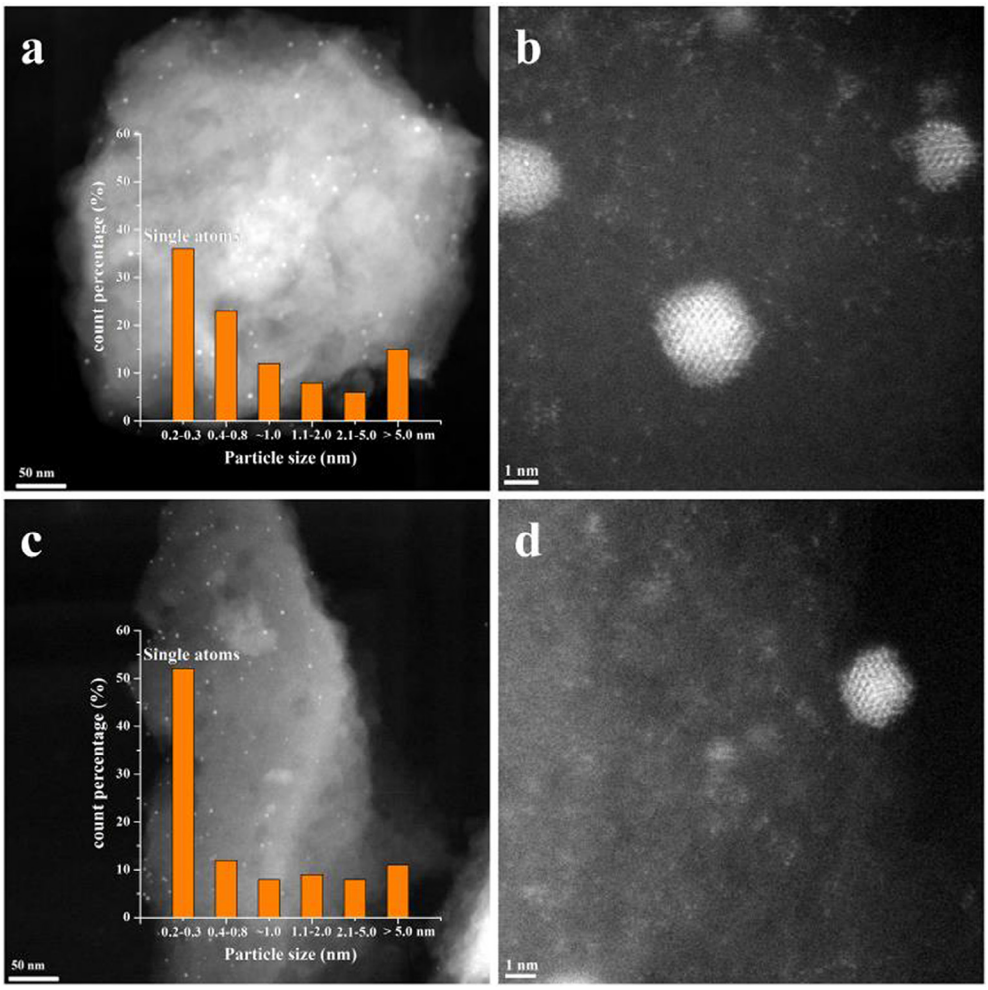

Fig. 1. Aberration-corrected HAADF-STEM images of the (a, b) Au/ROX08(AQ) and (c, d) Au/ROX08(AP) catalysts. The size distribution (inset) is based on over 200 observed Au species counted from the high-magnification images.

was detected, a deconvolution procedure was employed to establish the relative proportions of each species [26,27] (Fig. 2). The XPS peak position and the areas obtained from the fitting of both Au-based catalysts are listed in Table 1. Due to the high reducibility of the activated carbon towards the cationic Au species, there is a quantity of Au^0 with an $Au4f_{7/2}$ signal at 84.2 eV in both fresh Au-based catalysts. Indeed, in reactions using nanostructured gold/carbon catalysts, the Au nanoparticles that form during catalyst preparation are spectator species in that most of the Au^0 species do not participate in the reaction [15]. In addition, some cationic Au^+ and Au^{3+} species with $Au4f_{7/2}$ signals located at 85.1–85.5 eV and 86.7 eV, respectively, are also detected. The relative high content (47.3%) of cationic $AuCl_x$ species presenting in the Au/ROX08(AP) catalyst indicates that the H_2O_2/HCl mixture as the impregnating solvent could also efficiently generate and stabilize the cationic Au sites. Recent work by Hutchings group has shown that the AuCl species are the main active sites for ethyne hydrochlorination because the reaction proceeds through the oxidative addition of HCl to AuCl followed by the addition of acetylene and reductive elimination of VCM [14]. The Au^{3+} sites are easily decomposed to more active Au^+ sites when the temperature is increased to only 160 °C [13].

The evolution of the oxidation state of Au was further investigated by H_2-TPR analysis. Fig. 3 shows the H_2-TPR profiles of the bare activated carbon as well as the Au/ROX08(AP) and Au/ROX08(AQ) catalysts. Two hydrogen consumption peaks can be

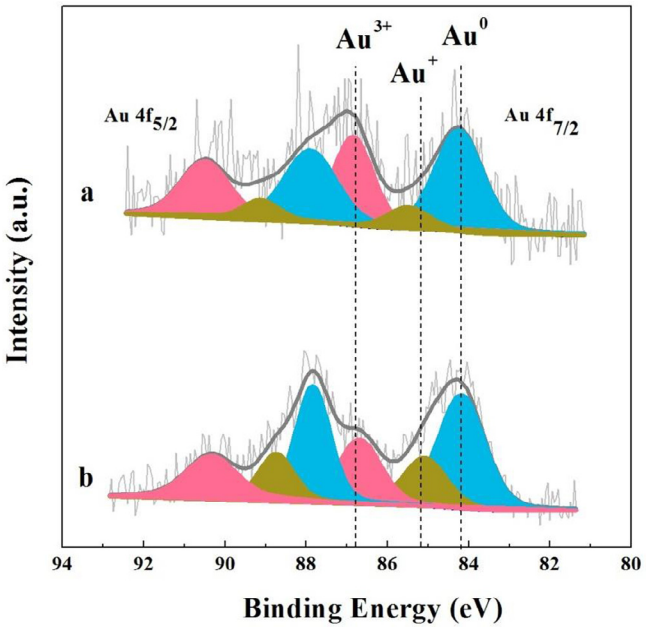

Fig. 2. XPS spectra and corresponding deconvolutions for the samples: (a) Au/ROX08(AP) and (b) Au/ROX08(AQ) catalysts.

Table 1
The relative contents of the Au species and binding energy of the Au-based catalysts.

Catalysts	Au species (%)			Binding energy (eV)		
	Au^{3+}	Au^0	Au^+	Au^{3+}	Au^0	Au^+
Au/ROX08(AP)	37.8	52.7	9.5	86.8	84.2	85.5
Au/ROX08(AQ)	27.3	52.3	20.4	86.7	84.2	85.1

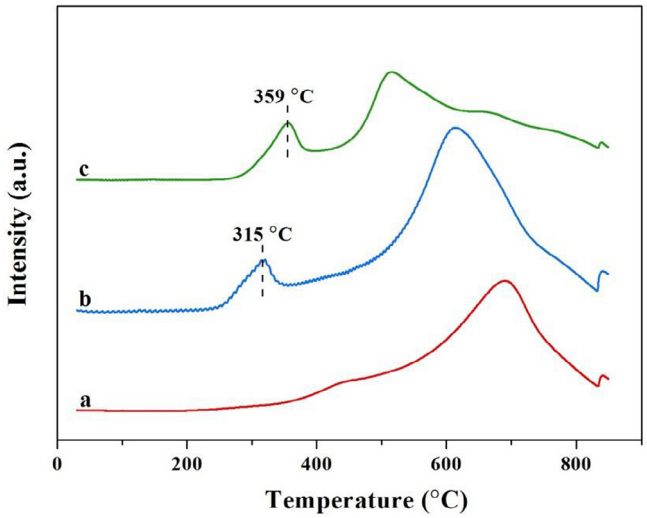

Fig. 3. TPR profiles of the (a) ROX08, (b) Au/ROX08(AQ) and (c) Au/ROX08(AP) catalysts.

seen in the TPR profiles of the Au/ROX08(AP) and Au/ROX08(AQ) samples. One is at a low temperature (280–360 °C) and the other is at a higher temperature (450–800 °C). The higher temperature peak can be assigned to the reduction of the SOGs on the carbon surface along with the concomitant release of CO and CO_2 [28,29]. Regarding the XPS analysis data, the low temperature hydrogen consumption peak could be attributed to the reduction of cationic Au species [30,31]. Furthermore, a temperature increase in the reduction band of cationic Au species to 359 °C is found for Au/ROX08(AP) (Fig. 3c). The higher reduction temperature (upward shift of 44 °C) of the Au/ROX08(AP) catalyst compared to Au/ROX08(AQ) (Fig. 3b) shows that the H_2O_2/HCl mixture as an impregnation solvent inhibits the reduction of cationic Au species. The stronger interactions between the cationic Au species and the SOGs make them more difficult to reduce.

3.2. Study of support chemistry and the Au-C interface

The chemistry of the supports plays an important role in determining the metal particle size and dispersion since the nucleation and growth processes during catalyst preparation are controlled by the nature of the support [32,33]. To elucidate the effect of the SOGs on the gold deposition and nucleation induced by using different impregnation solvents, TPD analysis was used since it is suitable for characterizing the nature of the SOGs based on the type and amount of gasses released (CO, CO_2 and H_2O) at different decomposition temperatures [34,35], as seen in Fig. 4a.

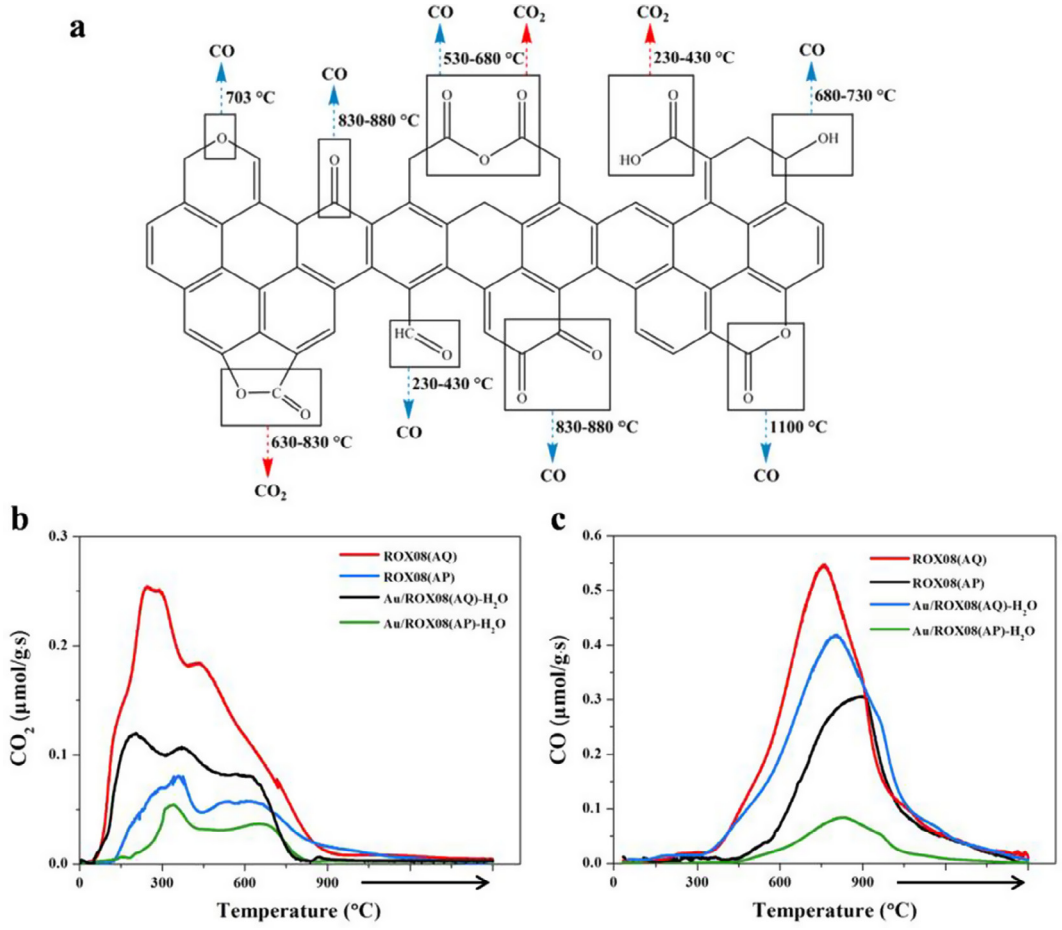

Fig. 4. (a) SOGs and specific sites generally present on the carbon surface. The arrows show the decomposition product(s) based on the TPD deconvolution spectra. Spectra of (b) CO_2 and (c) CO evolved in the TPD-MS of the ROX08(AQ), ROX08(AP), Au/ROX08(AQ)-H_2O and Au/ROX08(AP)-H_2O samples.

Fig. 4b and 4c show the CO_2 and CO TPD-MS spectra of *aqua regia*- and H_2O_2/HCl mixture-treated AC samples, respectively. The pristine activated carbon has a very low SOG content, as revealed by the small amounts of CO and CO_2 evolved (Fig. S4). Oxidation by *aqua regia* or the H_2O_2/HCl mixture incorporates a high content of SOGs onto the activated carbon, as shown by the large increase in the amounts of CO and CO_2 released (Tables 2 and 3). In particular, the CO_2 spectrum (Fig. 4b) shows that ROX08(AQ) has high contents of carboxyl groups and carboxylic anhydrides while lactones are present in lower amounts. In contrast, as shown in Table 2, the total amount of CO_2 released from ROX08(AP) is 152.1 μmol/g, which is 226.7 μmol/g less than that released from ROX08(AQ), suggesting that the ROX08(AP) has lower contents of carboxyl groups, carboxylic anhydrides and lactones than ROX08(AQ). On the other hand, as shown in Fig. 4c and Table 3, a large amount of phenol and carbonyl groups (639.2 μmol/g) are successfully incorporated by using the H_2O_2/HCl mixture, and the resulting content is much higher than that seen in ROX08(AQ) (177.0 μmol/g). Previously, Bulushev et al. [36] reported that phenolic groups interact with the Au^{3+} precursor by anchoring the cationic Au species. Interactions between the Au^{3+} precursor and the carboxylic groups leads to surface decarboxylation and reduction of Au^{3+} to Au^0. Actually, the cationic gold species are expected to be completely reduced to metallic gold clusters. While, the cationic Au species can be formed and stabilized either on the carbonaceous materials nor the metal oxide surface with the specific type of hydroxyl groups [37]. Indeed, such synergism between the Au and the support seems to be an essential factor in Au catalysis, which mainly attributes to the generation and stabilization of cationic Au species on the support. Thus, to further study of the Au-C interface and the influence of SOGs on Au deposition, TPD-MS analysis was also performed on Au/ROX08(AQ)-H_2O and Au/ROX08(AP)-H_2O catalysts that were prepared by impregnation in deionized water. The data obtained for the Au/ROX08(AP)-H_2O and Au/ROX08(AQ)-H_2O catalysts are presented in Fig. 4 and Tables 2 and 3. For CO_2 evolution (Fig. 4b), Au deposition on the ROX08(AQ) surface leads to the reduction of a large amount of the carboxyl groups, carboxylic anhydrides and lactones. However, for Au/ROX08(AP)-H_2O, we found that the CO_2 evolution profile is less affected by Au deposition. As far as the CO evolution profile, an obvious decrease in the intensity of the peak attributable to the phenol and carbonyl groups was noticed for Au/ROX08(AP)-H_2O upon gold deposition. For Au/ROX08(AQ)-H_2O, only a slightly decrease in the phenol and carbonyl groups was observed. Indeed, the amounts of CO evolved before and after gold deposition were 639.2 μmol/g (CO, ROX08(AP)), 149.1 μmol/g (CO, Au/ROX08(AP)-H_2O), 799.8 μmol/g (CO, ROX08(AQ)), and 643.1 μmol/g (CO, Au/ROX08(AQ)-H_2O). The metal deposition may contribute to the significant decrease in the surface oxygen released upon decomposition or surface reconstruction. In addition, the functionalized surface sites on the activated carbon may anchor some single atoms before they aggregate into larger particles [38]. Considering the TPD-MS and STEM analyses performed on the Au/ROX08(AP)-H_2O catalyst in this study, it is more likely that the active sites are isolated cationic Au species directly bonded to phenol and carbonyl groups created by the H_2O_2/HCl mixture. In contrast, gold may be grafted by all the SOGs, particularly by the carboxyl groups, carboxylic anhydrides and lactones groups, for Au/ROX08(AQ)-H_2O catalyst. As mentioned above, lower concentrations of ethers, carboxyl groups, carboxylic anhydrides and lactones with higher concentrations of phenol and carbonyl groups on ROX08(AP) than on ROX08(AQ) may make it a more appropriate carbon support for the anchoring and stabilization of atomically dispersed cationic Au sites. These data show that support chemistry plays an important role in determining catalyst particle size and dispersion since the nucleation and growth processes during catalyst preparation are resolved by the nature of the support.

3.3. Catalytic study of ethyne hydrochlorination

Au^{3+} species can efficient activate carbon-carbon triple bonds, making them suitable homogeneous catalysts for many organic synthesis reactions [39]. The catalytic performance of Au-based catalysts for ethyne hydrochlorination is shown in Fig. 5. As seen for the solo Au-based catalysts prepared using either H_2O_2 or HCl, the maximum conversions of ethyne are only 52.1% and 79.6%, respectively. In contrast, the gold/carbon catalyst prepared using the H_2O_2/HCl mixture showed higher activity with an ethyne conversion of 89.3%. Compared to the most effective Au/ROX08(AQ) reference catalyst prepared using *aqua regia* (C_2H_2 conversion = 85.6%), the Au/ROX08(AP) show even higher activity. Notably, the higher activity of the Au/ROX08(AP) catalyst is likely due to the abundance of atomically dispersed cationic Au sites.

Table 2
Amount and decomposition temperatures of different SOGs and the total amount of SOGs (obtained from the deconvolution of the CO_2-TPD curves).

Sample	Peak 1[a] Carboxyl	Peak 2 Carboxylic anhydride	Peak 3 Peroxide	Peak 4 Lactone	Total
ROX08(AQ)	141.0	147.8	/[b]	90.0	378.8
ROX08(AP)	62.1	8.9	/	81.1	152.1
Au/ROX08(AQ)-H_2O	41.9	111.8	/	47.7	201.4
Au/ROX08(AP)-H_2O	42.1	7.3	/	44.7	94.1

[a] The amount of SOGs in μmol/g.
[b] There is no such surface oxygenated group present on the activated carbon according to the results of deconvolution.

Table 3
Amount and decomposition temperatures of different SOGs and the total amount of SOGs (obtained from the deconvolution of the CO-TPD curves).

Sample	Peak 1[a] Adsorptive CO	Peak 2 Carboxylic anhydride	Peak 3 phenol	Peak 4 ether	Peak 5 carbonyl	Total
ROX08(AQ)	/[b]	/	7.3	622.8	169.7	799.8
ROX08(AP)	/	/	109.6	/	529.6	639.2
Au/ROX08(AQ)-H_2O	/	/	4.7	520.3	118.1	643.1
Au/ROX08(AP)-H_2O	/	/	96.2	/	52.9	149.1

[a] The amount of SOGs in μmol/g.
[b] There is no such surface oxygenated group present on the activated carbon according to the results of deconvolution.

In addition, the C_2H_2 conversion by Au/ROX08(AP) remained at a high and steady level (>83.3%), as shown in Fig. 5a. We only observed a slight decrease in conversion (6.0%) at 1480 h^{-1} after 12 h. In contrast, the Au/ROX08(AQ) reference catalyst and the Au/ROX08(A) and Au/ROX08(P) catalysts show rapid deactivation over the first few hours and then a slower decay over the remainder of the reaction. These results suggest that the Au/ROX08(AP) catalyst has better activity and stability than the traditional Au-based catalyst made with *aqua regia*. Considering the catalytic performance, process safety requirements and environmental impact, the H_2O_2/HCl mixture is an optimal impregnation solvent for the preparation of gold/carbon catalysts. Control tests with different impregnation solvent-treated carbon materials (ROX08(AP), ROX08(AQ), ROX08(A), ROX08(P) and ROX08) showed lower ethyne conversions (below 8%) (Fig. S5). Remarkably, the selectivity for VCM is above 99.9% with only trace amounts (<0.1%) of 1, 2-dichlorethane and chlorinated oligomers observed in the current study (Fig. 5b).

To further evaluate the H_2O_2/HCl mixture preparation protocol for low-content Au/C catalysts, a series of fresh Au/C species with different Au contents (0.1, 0.3, 0.5 wt%) were prepared using the same protocol as that used for Au/ROX08(AP), and their catalytic activities were tested. As seen in Fig. 6, the conversion of C_2H_2 decreased with decreasing Au content, but the 0.1 wt% Au/ROX08 (AP) catalyst still exhibits a high and stable catalytic performance. Based on the flow conditions and the amount of catalyst employed, the 0.1 wt% Au/ROX08(AP) catalyst has a space-time yield (STY) of 946 kg VCM/(kg Au h), which is slightly higher than that of the commercial $Na_3Au(S_2O_3)_2$/C catalysts (ranged from 150 to 850 kg VCM/(kg Au h)) [18]. This superior activity allows the Au loading to be decreased to an extremely low level while maintaining satisfactory productivity using the H_2O_2/HCl mixture preparation methods.

We also investigated the interactions of the gold with the SOGs created by the acid treatment and the magnitude of their impact on the catalyst activity, since they may be possible anchoring sites for Au on the carbon surface and the support may play a crucial role in ethyne hydrochlorination. The results indicate that high activities with approximately 72% conversion can still be achieved with the Au/ROX08(AP)-H_2O catalyst prepared in the deionized water using the H_2O_2/HCl mixture-pretreated ROX08 carbon (Fig. 7), and this activity is only slightly lower than that of the Au/ROX08(AP) catalysts. In contrast, the Au/ROX08(AQ)-H_2O catalyst has a significantly lower activity than that of the catalyst prepared in *aqua regia* and the Au/ROX08(AP)-H_2O catalysts. Note that the catalysts prepared with deionized water on the untreated ROX08 carbon without SOGs are completely inactive. The testing results show that to generate an active catalyst, the atomic gold must be linked to surface oxygen ligands, and the SOGs being merely present on the carbon support is not sufficient. This experimental result is important because it sheds light on the role of the oxygen in the form of SOGs on the final catalyst activity and stability of the catalyst. It seems that the effect of the impregnation solvent on the carbon support rather than gold itself is the more significant factor in determining the activity and stability of the catalyst. In light of the TPD-MS and XPS analysis performed in this study, we thus propose cationic gold (AuCl) species stabilized by specific types of SOGs via -O- linkages are the active sites for the ethyne hydrochlorination. It is clear that the H_2O_2/HCl mixture can create more favorable carbon surface chemistry than *aqua regia*-based preparation methods for the Au/AC catalysts.

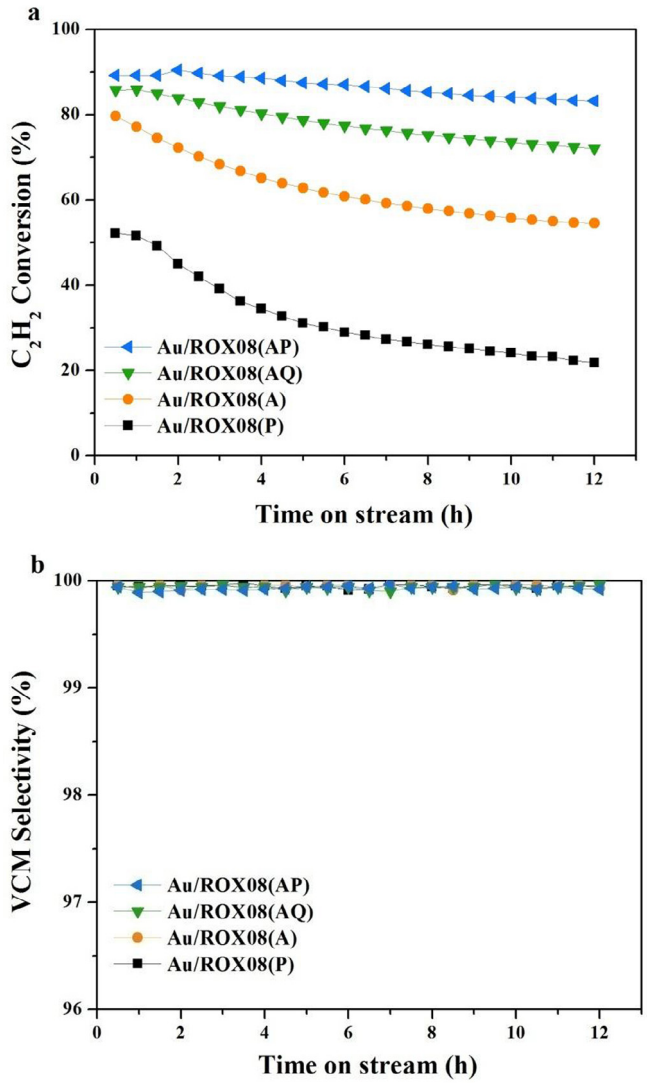

Fig. 5. Conversion of ethyne into VCM in acetylene hydrochlorination over Au/ROX08(AP), Au/ROX08(AQ), Au/ROX08(A) and Au/ROX08(P) catalysts. Reactions were carried out at 180 °C, atmospheric pressure, a space velocity GHSV(C_2H_2) of 1480 h^{-1}, and HCl/C_2H_2 = 1.2/1.

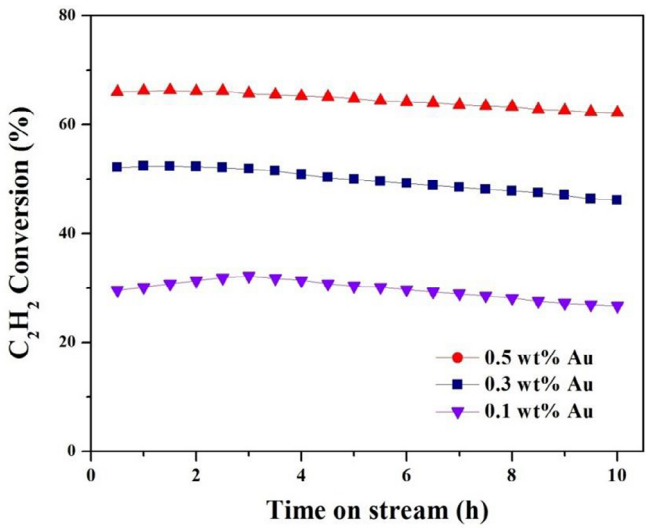

Fig. 6. Catalytic activity of Au/ROX08(AP) as a function of Au loading. Reactions were carried out at 180 °C, atmospheric pressure, a space velocity GHSV(C_2H_2) of 1480 h^{-1}, and HCl/C_2H_2 = 1.2/1.

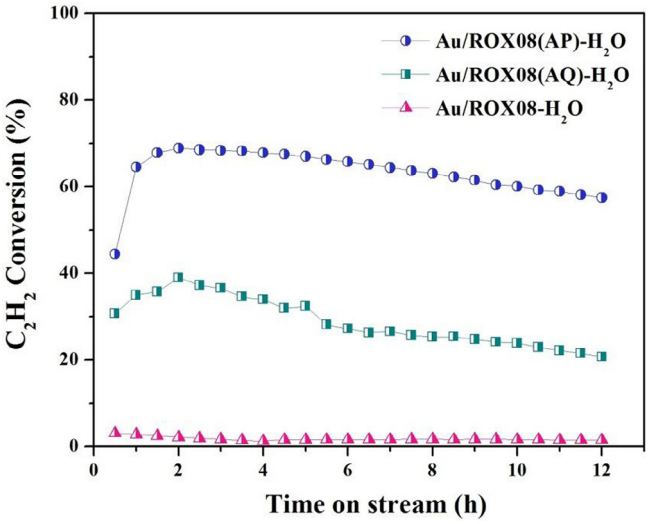

Fig. 7. Catalytic activity of catalysts prepared in water with impregnation solvent-treated or untreated carbon supports. Reactions were carried out at 180 °C, atmospheric pressure, a space velocity GHSV(C_2H_2) of 1480 h^{-1}, and HCl/C_2H_2 = 1.2/1.

3.4. Reaction mechanisms of ethyne hydrochlorination catalyzed by SOGs stabilized single-site Au sites

To determine if the active Au sites in the ethyne hydrochlorination catalysts are atomic cationic species anchored through -O- ligands, we used DFT calculations. Here, we focus on carbonyl groups because the H_2O_2/HCl mixture generates a significant amount of carbonyl groups on the carbon materials, and other SOGs such as carboxyl groups, carboxylic anhydrides and lactones are less affected by Au deposition. In addition, the highly dispersed Au(I) species are crucial for this reaction and species in a similar oxidation state are responsible for the activity of these catalyst systems. Thus, here we focus on Au(I) by investigating AuCl on a graphite surface cut along the (1 1 9) index plane, and the AuCl is absorbed on the oxygen atom of a carbonyl and a carbon atom of a benzene ring, respectively. Fig. S6 shows that adsorption energy of AuCl onto the oxygen atom of carbonyl (−318.1 kJ/mol) is much lower than that of AuCl on a graphite surface cut along the (1 1 9) index plane (−285.2 kJ/mol). The adsorption energy differences for various adsorption configurations show that AuCl tends to favor the oxygen atoms on carbonyl interacting through a Au-O bond. Hence, we only explored reaction mechanisms of AuCl with single SOGs such as carbonyl, as displayed in Fig. 8.

The most stable configuration of the interaction of HCl with a carbonyl group-stabilized AuCl has a binding energy of −30.4 kJ mol^{-1}, which is comparable to that for $AuCl_2H$ (−17.9 kJ mol^{-1}) (Fig. 8a). Hirshfeld charge analysis showes that the positive charge (+0.31 e) of $AuCl_2H$ is similar to that for Au^{3+} (0.41e) (Fig. 8b). The VCM can be generated by $AuCl_2(C_2H_3)$, which is more stable than $AuCl_2H(C_2H_2)$ with binding energies of −288.1 kJ mol^{-1} versus −25.5 kJ mol^{-1} (Fig. 8a). VCM is further stabilized with a binding energy of −294.6 kJ mol^{-1}, but this can be disrupted by the presence of HCl. Compared with AuCl on a graphite surface [14], based on the adsorption strength, HCl interacts weakly with carbonyl group-stabilized AuCl (−17.9 kJ mol^{-1} v.s. −73 kJ mol^{-1}); however, the latter active species interacts more strongly with C_2H_2 reactants (−288.1 kJ mol^{-1} v.s. −224 kJ mol^{-1}), which facilitates the adsorption of C_2H_2 and hence the reaction.

3.5. Catalyst regeneration and catalytic cycle

Although Au catalysts are highly active initially, they undergo fast deactivation [18]. Therefore, identifying methods to stabilize or reactivate the catalysts is of great importance. Goguet et al. [40] demonstrated that large particles of gold/carbon can be

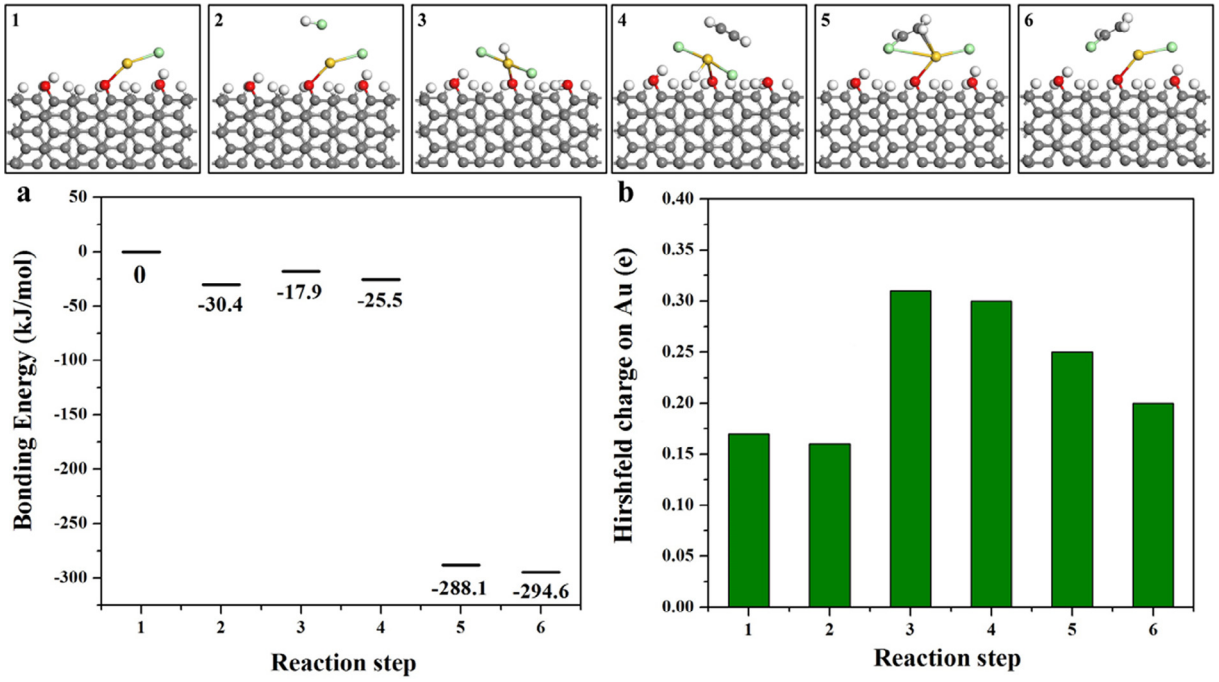

Fig. 8. Evaluation of catalytic activity by DFT calculations. (a) The bar chart shows binding energies for each energy minima and (b) the Hirshfeld charge on each Au atom. The given energies are referenced to the geometry-optimized configuration of AuCl stabilized by carbonyl groups on the carbon support and gas phase C_2H_2 and HCl. Gray balls represent carbon atoms, red balls represent oxygen atoms, yellow balls represent gold atoms, light green balls represent chlorine atoms and white balls represent hydrogen atoms.

redispersed in the presence of methyl iodide during the carbonylation of methanol to methyl acetate under harsh conditions (240 °C and 16 bar). In previous studies on catalyst reactivation for the hydrochlorination of acetylene, the activity of a 1% Au/C catalyst that deactivated during the reaction can be revived to an extent by off-line treatment with *aqua regia* [41]. Thus, further investigations are needed to prove the effectiveness of treatment with an H_2O_2/HCl mixture for regenerating the catalytic activity of deactivated catalysts.

Fig. 9a shows the ex situ X-ray powder diffraction patterns obtained during treatment with the H_2O_2/HCl mixture at 70 °C for 60 min. The results obtained show that the diffraction peaks associated with metallic Au^0 species disappear, and only carbon diffraction peaks are found for the Au/ROX08(AP)-R sample, which is consistent with the fact that the Au particles disperse into smaller species. HAADF-STEM analysis demonstrated that the used Au/ROX08(AP) sample contained large Au particles with relatively large sizes of 8–10 nm, suggesting some of the Au particles/clusters aggregated (Fig. 9b). After the treatment, the gold is essentially distributed as isolated Au atoms (46% of the gold counted in the images was present as isolated atoms) although a small number of Au dimers and subnanometer Au clusters are also present (Fig. 9c-d). Moreover, the XPS characterization of the used Au/ROX08(AP) and Au/ROX08(AP)-R catalysts show that the high number of Au^0 species were oxidized to cationic Au species when the used Au/ROX08(AP) was treated with the H_2O_2/HCl mixture (the $AuCl_x$ content increased from 30.4% to 67.1%). A small number of particles containing both Au and Cl were observed by elemental mapping analysis, which showed that the Au and Cl signals are uniformly displayed (Fig. S7). In addition, ICP analysis show that the contents of Au (0.95 wt%) in the regenerated catalysts are nearly equal to the nominal total metal loading of 1 wt% impregnated onto the support initially. These results confirm that once the Au is deposited on the carbon surface, subsequent treatments with the H_2O_2/HCl mixture were not capable of dissolving the gold from the carbon support; instead, the treatments simply reoxidize the gold. In terms of oxidation chemistry, H_2O_2 has a very high oxidizing potential (Table 4). The potential of H_2O_2 (1.78 V) is significantly higher than those of Au^{3+} (1.52 V) and Au^+ (1.69 V), which enables the oxidization of Au^0 to $AuCl_x$. Here, we present direct evidence for the latter from the XPS and UV–vis analyses, which indicate that the H_2O_2/HCl mixture can dissolve Au^0 into $AuCl_4^-$ (Fig. S8). In addition, it is possible that the Cl atoms may spontaneously adsorb onto the surface of the Au particles because of the high potential energy of the small particles or even coordination with the Au^0 particles [42]. The potential of gold may decrease, and the Au particles may be oxidized more easily by reacting with H_2O_2 to form Au-Cl species, which was revealed by the XPS and EDS elemental mapping analyses.

To determine if the used catalyst had regained its catalytic activity after treatment with the H_2O_2/HCl mixture, the regenerated Au/ROX08(AP) catalysts were evaluated. To deactivate the catalysts, the reaction was performed at an extremely high reaction temperature (210 °C) and a high C_2H_2 GHSV (3000 h^{-1}). Constant deactivation of the fresh Au/ROX08(AP) catalysts occurred throughout the reaction (Fig. 10). However, the catalytic activity of the deactivated Au/ROX08(AP) catalyst could almost be regenerate after treatment with the H_2O_2/HCl mixture, and the ethyne conversion is only slightly lower than that achieved with the fresh catalyst. In addition, the Au/ROX08(AP) catalyst after treatment

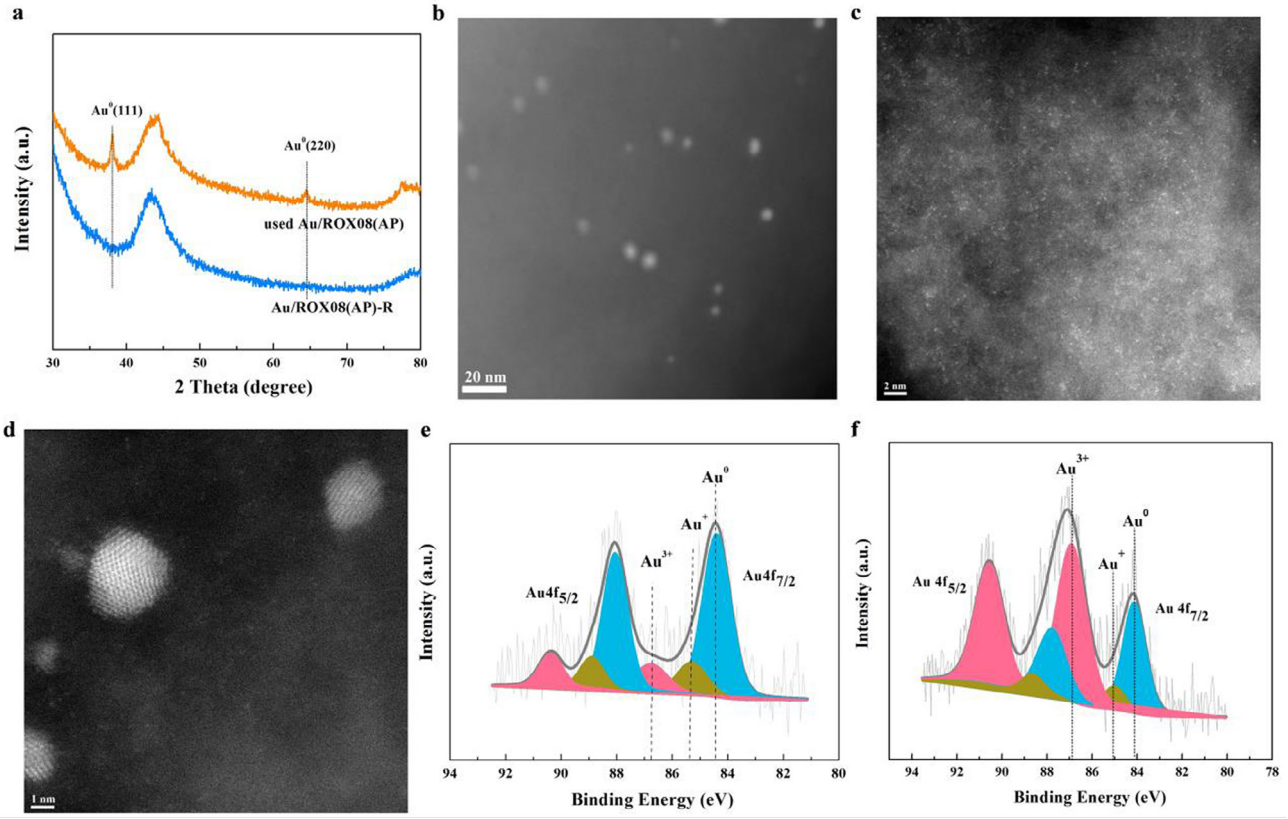

Fig. 9. Structural characterizations of used Au/ROX08(AP) and regenerated Au/ROX08(AP)-R catalyst. (a) Ex situ X-ray powder diffraction patterns. (b) Representative STEM-HAADF image of the used Au/ROX08(AP) catalyst. (b and c) STEM-HAADF image of the regenerated Au/ROX08(AP)-R catalyst. Au 4f XPS spectra of (e) the used Au/ROX08(AP) catalyst and the regenerated Au/ROX08(AP)-R catalyst.

Table 4
Related half-reactions and the corresponding electric potentials.

Half-reaction	Electric potential (V)
$Au^{3+} + 3e^- = Au$	1.52
$AuCl_4^- + 3e^- = Au + 4Cl^-$	0.93
$Au^+ + e^- = Au$	1.69
$AuCl_2^- + e^- = Au + 2Cl^-$	1.15
$H_2O_2 + 2H^+ + 2e^- = 2H_2O$	1.78

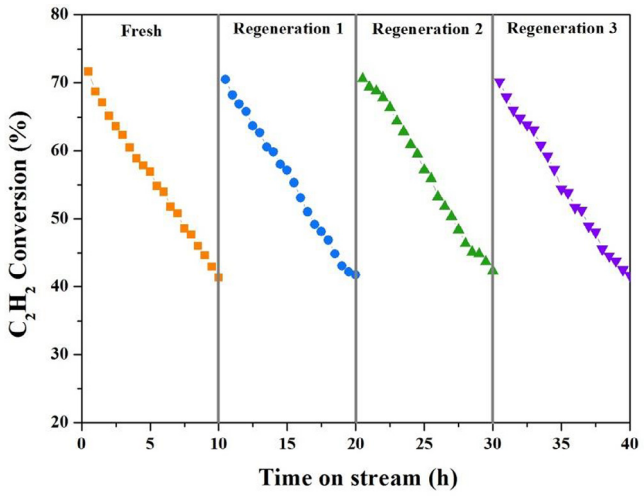

Fig. 10. Durability and activity for ethyne hydrochlorination of the fresh Au/ROX08 (AP) catalyst and the used Au/ROX08(AP) catalyst regenerated with the H_2O_2/HCl mixture treatment for 3 cycles. Reactions were carried out at 210 °C, atmospheric pressure, a space velocity GHSV(C_2H_2) of 3000 h^{-1}, and HCl/C_2H_2 = 1.2/1.

with the H_2O_2/HCl mixture can be recycled through several deactivation/regeneration cycles with a negligible decrease in catalytic performance.

4. Conclusion

In summary, we presented a simple and green methodology for the preparation of Au/AC catalysts using a H_2O_2/HCl mixture. The catalytic results showed that the Au/ROX08(AP) catalyst presented a higher conversion than the Au/ROX08(AQ) catalyst, which was prepared using an impregnation method with traditional *aqua regia* as the solvent, in the hydrochlorination of ethyne. After careful characterization of the Au/ROX08(AP) and Au/ROX08(AQ) catalysts by a combination of XPS, H_2-TPR and TPD analyses with direct STEM imaging, we found that the improved catalytic performance could be attributed to the enhanced dispersion of Au and the stabilization of atomically dispersed $AuCl_x$ active species by specific types of SOGs (such as carbonyl groups) created by the H_2O_2/HCl mixture via -O- linkages. The presence of the surface oxygen ligands is important for the formation of active Au sites. The conclusions drawn about the effects of SOGs on the composition and structure of the single-site cationic AuCl species catalyst were also supported by DFT calculations. However, the role of different defect sites on the carbon surface could not be completely ruled out and would require further systematic investigation. In addition, the Au/AC catalysts can maintain their activity through several deactivation/regeneration cycles with negligible changes in catalytic performance by treatment with the H_2O_2/HCl mixture since the mixture can reoxidize bulk Au^0 species to expose their active cationic Au sites. As well as being interesting by itself, the synthesis methodology described herein also provides a blueprint for the green synthesis of various other carbon-supported high-valent metal catalysts.

Acknowledgements

Financial support from the National Natural Science Foundation of China (NSFC; grant No. 21606199, 21476207) are gratefully acknowledged.

References

[1] G.J. Hutchings, J. Catal. 96 (1985) 292–295.
[2] M. Haruta, T. Kobayashi, H. Sano, N. Yamada, Chem. Lett. 16 (1987) 405–408.
[3] J. Guzman, B.C. Gates, J. Am. Chem. Soc. 126 (2004) 2672–2673.
[4] M. Yang, S. Li, Y. Wang, J.A. Herron, Y. Xu, L.F. Allard, S. Lee, J. Huang, M. Mavrikakis, M. Flytzani-Stephanopoulos, Science 346 (2014) 1498–1507.
[5] R. Ciriminna, E. Falletta, C.D. Pina, J.H. Teles, M. Pagliaro, Angew. Chem. Int. Ed. 55 (2016) 14210–14217.
[6] C.J. Davies, P.J. Miedziak, G.L. Brett, G.J. Hutchings, Chin. J. Catal. 37 (2016) 1600–1607.
[7] T. Risse, S. Shaikhutdinov, N. Nilius, M. Sterrer, H.-J. Freund, Acc. Chem. Res. 39 (2008) 949.
[8] L. Prati, A. Villa, A.R. Lupini, G.M. Veith, PCCP 14 (2012) 2969–2978.
[9] K. Jiang, A. Eitan, L.S. Schadler, P.M. Ajayan, R.W. Siegel, Nano Lett. 3 (2003) 275–277.
[10] B.F. Machado, M. Oubenali, M.R. Axet, T.T. Nguyen, M. Tunckol, M. Girleanu, O. Ersen, I.C. Gerber, P. Serp, J. Catal. 309 (2014) 185–198.
[11] J. Xu, J. Zhao, J. Xu, T. Zhang, X. Li, X. Di, J. Ni, J. Wang, J. Cen, Ind. Eng. Chem. Res. 53 (2014) 14272–14281.
[12] M. Haruta, S. Tsubota, T. Kobayashi, H. Kageyama, M.J. Genet, B. Delmon, J. Catal. 144 (1993) 175–192.
[13] M. Conte, C.J. Davies, D.J. Morgan, T.E. Davies, D.J. Elias, A.F. Carley, P. Johnston, G.J. Hutchings, J. Catal. 297 (2013) 128–136.
[14] G. Malta, S.A. Kondrat, S.J. Freakley, C.J. Davies, L. Lu, S. Dawson, A. Thetford, E. K. Gibson, D.J. Morgan, W. Jones, P.P. Wells, P. Johnston, C.R.A. Catlow, C.J. Kiely, G.J. Hutchings, Science 355 (2017) 1399–1403.
[15] M. Conte, C.J. Davies, D.J. Morgan, T.E. Davies, A.F. Carley, P. Johnston, G.J. Hutchings, Catal. Sci. Technol. 3 (2013) 128–134.
[16] G. Malta, S.J. Freakley, S.A. Kondrat, G.J. Hutchings, Chem. Commun. 53 (2017) 11733–11746.
[17] J. Zhao, B. Wang, X. Xu, Y. Yu, S. Di, H. Xu, Y. Zhai, H. He, L. Guo, Z. Pan, X. Li, J. Catal. 350 (2017) 149–158.
[18] P. Johnston, N. Carthey, G.J. Hutchings, J. Am. Chem. Soc. 137 (2015) 14548–14557.
[19] X. Liu, M. Conte, D. Elias, L. Lu, D.J. Morgan, S.J. Freakley, P. Johnston, C.J. Kiely, G.J. Hutchings, Catal. Sci. Technol. 6 (2016) 5144–5153.
[20] M.D. Segall, J. Phys.: Condens. Matter 14 (2002) 2957–2973.
[21] N. Govind, M. Petersen, G. Fitzgerald, D. King-Smith, J. Andzelm, Comput. Mater. Sci. 28 (2003) 250–258.
[22] J.P. Perdew, K. Burke, M. Ernzerhof, Phys. Rev. Lett. 77 (1996) 3865–3868.
[23] D.R. Hamann, M. Schlüter, C. Chiang, Phys. Rev. Lett. 43 (1979) 1494–1497.
[24] K.C. O'Connell, J.R. Monnier, J.R. Regalbuto, Appl. Catal. B: Environ. 225 (2018) 264–272.
[25] J. Gu, Q. Du, Y. Han, Z. He, W. Li, J.L. Zhang, PCCP 16 (2014) 25498–25507.
[26] J. Zhao, J. Xu, J. Xu, T. Zhang, X. Di, J. Ni, X. Li, Chem. Eng. J. 262 (2015) 1152–1160.
[27] J. Zhao, Y. Yu, X. Xu, S. Di, B. Wang, H. Xu, J. Ni, L. Guo, Z. Pan, X. Li, Appl. Catal. B: Environ. 206 (2017) 175–183.
[28] S. De Miguel, O. Scelza, M. Román-Martınez, C. Salinas-Martınez de Lecea, D. Cazorla-Amorós, A. Linares-Solano, Appl. Catal. A: Gen. 170 (1998) 93–103.
[29] J. Figueiredo, M. Pereira, M. Freitas, J. Orfao, Carbon 37 (1999) 1379–1389.
[30] M. Conte, C.J. Davies, D.J. Morgan, A.F. Carley, P. Johnston, G.J. Hutchings, Catal. Lett. 144 (2014) 1–8.
[31] K. Zhou, W. Wang, Z. Zhao, G. Luo, J.T. Miller, M.S. Wong, F. Wei, ACS Catal. 4 (2014) 3112–3116.
[32] F. Coloma, A. Sepúlveda-Escribano, J.L. Fierro, F. Rodríguez-Reinoso, Appl. Catal. A: Gen. 150 (1997) 165–183.
[33] J.K. Edwards, B. Solsona, E. Ntainjua, A.F. Carley, A.A. Herzing, C.J. Kiely, G.J. Hutchings, Science 323 (2009) 1037–1041.
[34] J. Zhou, Z. Sui, J. Zhu, P. Li, D. Chen, Y. Dai, W. Yuan, Carbon 45 (2007) 785–796.
[35] J.L. Figueiredo, M.F. Pereira, M.M. Freitas, J.J. Órfão, Carbon 37 (1999) 1379–1389.
[36] D.A. Bulushev, I. Yuranov, E.I. Suvorova, P.A. Buffat, L. Kiwi-Minsker, J. Catal. 224 (2004) 8–17.
[37] M.A. Brown, Y. Fujimori, F. Ringleb, X. Shao, F. Stavale, N. Nilius, M. Sterrer, H.-J. Freund, J. Am. Chem. Soc. 133 (2011) 10668–10676.
[38] E. Auer, A. Freund, J. Pietsch, T. Tacke, Appl. Catal. A: Gen. 173 (1998) 259–271.
[39] A.S. Hashmi, Gold Bull. 37 (2004) 51–65.
[40] A. Goguet, C. Hardacre, I. Harvey, K. Narasimhara, Y. Saih, J. Sa, J. Am. Chem. Soc. 131 (2009) 6973–6975.
[41] M. Conte, A.F. Carley, G.J. Hutchings, Catal. Lett. 124 (2008) 165–167.
[42] X. Duan, Y. Yin, X. Tian, J. Ke, Z. Wen, J. Zheng, M. Hu, L. Ye, Y. Yuan, Chin. J. Catal. 37 (2016) 1794–1803.